Image Compressive Sensing Using Overlapped Block Projection and Reconstruction

Sheng Shi[1], Ruiqin Xiong[1], Siwei Ma[1], Xiaopeng Fan[2] and Wen Gao[1]
[1] Institute of Digital Media, Peking University, Beijing 100871, China
[2] Department of Computer Science, Harbin Institute of Technology, Harbin 150001, China
Email: {shshi, rqxiong, swma, wgao}@pku.edu.cn, fxp@hit.edu.cn

***Abstract*—Compressive sensing allows a signal to be sampled at sub-Nyquist rate and still get recovered exactly, if the signal is sparse in some domain. Block compressive sensing (BCS) is advocated for practical image compressive sensing, since it processes image at block level and significantly reduces the memory requirement for storing projection matrix. However, existing BCS methods process blocks separately, which breaks the continuity between blocks and usually produces blocking artifacts. This paper proposes a new image compressive sensing scheme using overlapped-block projection and reconstruction (OBPR), in which the sampling is performed on overlapped blocks. During reconstruction, the sparsity constraint in transform domain is also enforced on the overlapped blocks. An augmented Lagrangian method is used to solve the optimization problem efficiently. Experimental results show that the proposed OBPR scheme achieves significantly better results than the existing BCS schemes in reconstruction quality.**

I. Introduction

Compressive sensing (CS) [1] [2] [3] theory is a new signal processing theory, which allows a signal to be sampled at sub-Nyquist rate via linear projection onto a random basis and still get recovered exactly, if the signal is sparse in some domain. More specifically, suppose that we want to recover signal $\mathbf{x}$ with length N from its measurement $\mathbf{y}$ with length $M(M \leq N)$, which is just the linear projection of $\mathbf{x}$, i.e.

$$\mathbf{y} = \Phi\mathbf{x}, \tag{1}$$

where Φ is an $M \times N$ measurement matrix with the measurement subrate being M/N. It is impossible to recover the signal $\mathbf{x} \in R^N$ from the observation $\mathbf{y} \in R^M$ in general. However, if $\mathbf{x}$ is sufficiently sparse in some domain, then exact recovery is possible–this is the fundamental tenet of CS theory.

Obviously, the dimensionality of the CS sampling process grows quickly as the size of $\mathbf{x}$ increases, which leads to huge memory requirement for storing the sampling matrix Φ. Additionally, a large matrix brings heavy computational burden in the reconstruction process. One approach to solve the above issue is to break the image into small blocks and process each block separately. One such block-based CS (BCS) approach is proposed in [4]. However, since the blocks to be sampled are non-overlapped, existing BCS methods usually produce blocking artifacts, which greatly degrade the quality of the reconstructed image. In order to remove blocking artifacts, the BCS coupled with smoothed projected Landweber reconstruction (BCS-SPL) is proposed in [5]. BCS-SPL uses wiener filter to smooth the reconstructed image and obtains better performance than BCS [4]. However, wiener filter in BCS-SPL inevitably removes the details of the reconstructed image.

In this paper, we propose a new image compressive sensing scheme using overlapped block projection and reconstruction (OBPR). Different from traditional BCS and BCS-SPL, the sampling of image is applied on overlapped blocks. In process of reconstruction, we enforce the image sparsity in discrete cosine transform domain to improve the reconstruction quality. Furthermore, an efficient augmented Lagrangian based technique is exploited to solve the proposed optimization problem.

The rest of this paper is organized as follows. Section II describes the image compressive sensing method with overlapped block projection. Section III presents the corresponding reconstruction method. Section IV reports the simulation results for natural images followed by the conclusion in Section V.

This work was supported by the National Natural Science Foundation of China (61370114, 61322106, 61421062), Beijing Natural Science Foundation (4132039), Research Fund for the Doctoral Program of Higher Education (20120001110090) and also by Cooperative Medianet Innovation Center.

II. Image Compressive Sensing with Overlapped Block Projection

In traditional BCS, the blocks to be sampled cover different spatial position, that is to say, the blocks are non-overlapped. This leads to the loss of the correlation between pixels in different blocks, which may generate blocking artifacts in the reconstructed images. Therefore, the quality of the reconstructed image from BCS is usually unsatisfied. In order to remove blocking artifacts, BCS-SPL introduces wiener filter to smooth the reconstructed image and obtains better performance than BCS. However, the strength of filter is hard to determine. When the strength is small, the blocking artifacts can not be removed. With high strength of filter, not only the blocking artifacts but also the details of the reconstructed image are removed.

This paper proposes a new image compressive sensing scheme using overlapped block projection and reconstruction, where the sampling of an image is applied on overlapped blocks. Fig. 1 compares traditional non-overlapped block projection with overlapped block projection.

978-1-4799-8391-9/15/$31.00 ©2015 IEEE

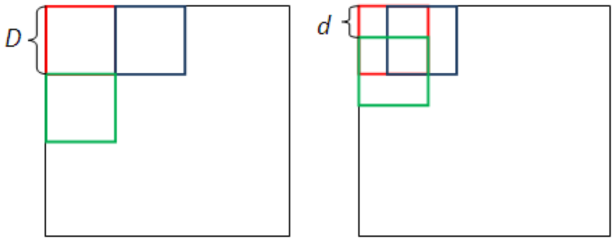

Fig. 1. Traditional block projection and overlapped block projection

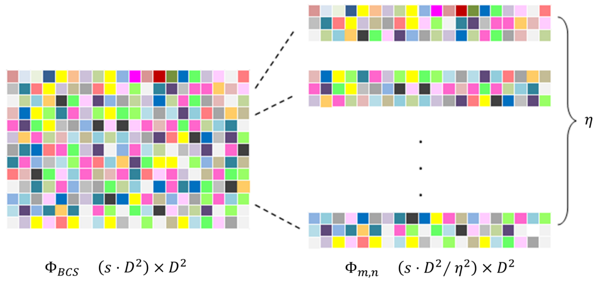

Fig. 2. The process of obtaining measurement matrices $\Phi_{m,n}$

In the sampling process of our proposed OBPR, we get blocks by distance d ($0<d<D$, $\mathrm{mod}(D,d)=0$) periodically as presented in Fig. 1. Suppose we have an image I (a two-dimensional grid) of size $H \times W$, where $I(i,j)$ denotes a pixel, and the indices i and j are the coordinates in the vertical and the horizontal directions, respectively. Suppose that the size of block is $D \times D$. Here, we use $B_{i,j}$ to denote a block, whose top left pixel is $I(i,j)$ [6] [7]. The complete set of block coordinates in image I is defined as:

$$\Omega_1 = \{(i,j) | 0 \le i \le H-D, 0 \le j \le W-D\}. \qquad (2)$$

Then, the complete set of blocks in image I is defined as:

$$\mathcal{B}_1 = \{B_{i,j} | (i,j) \in \Omega_1\}. \qquad (3)$$

In our OBPR sampling, the set of blocks is defined as:

$$\begin{aligned} \mathcal{B}_d &= \{B_{i,j} | (i,j) \in \Omega_d\} \\ \Omega_d &= \{(i,j) | \mathrm{mod}(i,d)=0, \mathrm{mod}(j,d)=0\}. \end{aligned} \qquad (4)$$

Further, the set of blocks $\mathcal{B}_d$ can be divided into η sets, η denotes overlap degree which is determined by d: $\eta = (D/d)^2$. In each set, the blocks are non-overlapped.

$$\begin{aligned} \mathcal{B}_d^{m,n} &= \{B_{i,j} | (i,j) \in \Omega_d^{m,n}\} \\ \Omega_d^{m,n} &= \{(i,j) | \mathrm{mod}(i,D) = md, \mathrm{mod}(j,D) = nd\} \\ &\text{where } m = 0,1,...D/d, \quad n = 0,1,...D/d. \end{aligned} \qquad (5)$$

In traditional BCS sampling, when measurement subrate is s, the size of measurement matrix is $(s \cdot D^2) \times D^2$. While in OBCS sampling, since the blocks are overlapped, in order to guarantee the same number of measurements, the size of measurement matrix is $(s \cdot D^2/\eta) \times D^2$.

Since the adjacent blocks have the similar information of image, if their measurement matrices are the same, the measurements will have many redundancies. In order to make the information of measurements more meanful, the overlapped blocks should have different measurement matrices. So, there should be η different measurement matrices $\Phi_{m,n}$ for η sets $\mathcal{B}_d^{m,n}$ respectively.

The η measurement matrices $\Phi_{m,n}$ can be obtained using the following steps. First, we generate a measurement matrix of size $(s \cdot D^2) \times D^2$ using the same method as that used in BCS and BCS-SPL. Then the matrix is divided into η submatrix of size $(s \cdot D^2/\eta) \times D^2$. This process is shown in Fig. 2.

To be clear, we define an operator $R_{i,j}$ which extracts the block $B_{i,j}$ from the input image $\mathbf{x}$. According to the equations $m = \mathrm{mod}(i,D)/d$ and $n = \mathrm{mod}(j,D)/d$, we can find the set $\mathcal{B}_d^{m,n}$ which includes block $B_{i,j}$. So the corresponding measurement matrix is $\Phi_{m,n}$. The image compressive sensing with overlapped block projection is described as below:

$$\mathbf{y}_{i,j} = \Phi_{m,n} R_{i,j} \mathbf{x}, \qquad (6)$$

where $(i,j) \in \Omega_d$, $\mathbf{y}_{i,j}$ is the measurement of block $B_{i,j}$.

III. Image Compressive Sensing with Overlapped Block Reconstruction

In reconstruction, we enforce the sparsity of image blocks in the complete set in discrete cosine transform domain. So the reconstruction can be presented as:

$$\begin{aligned} &\min_{\mathbf{x}} \textstyle\sum_{(p,q)\in\Omega_1} \|\Psi R_{p,q}\mathbf{x}\|_1 \\ &s.t.\ \mathbf{y}_{i,j} = \Phi_{m,n} R_{i,j}\mathbf{x}, \text{ for all } (i,j) \in \Omega_d, \end{aligned} \qquad (7)$$

where Ψ is DCT matrix.

Optimization problem (7) is quite difficult to solve directly due to the non-differentiability of sparsity item. Instead, making use of variable splitting technique [8] [9] [10], the problem becomes a constrained optimization:

$$\begin{aligned} &\min_{\mathbf{x}} \textstyle\sum_{(p,q)\in\Omega_1} \|\mathbf{w}_{p,q}\|_1 \\ &s.t. \mathbf{w}_{p,q} = \Psi R_{p,q}\mathbf{x}, \mathbf{y}_{i,j} = \Phi_{m,n} R_{i,j}\mathbf{x}, \text{for all } (i,j) \in \Omega_d \end{aligned} \qquad (8)$$

We employ augmented Lagrangian method to solve the function of (8):

$$\begin{aligned} L_A(\mathbf{w}_{p,q}, \mathbf{x}) &= \sum_{(p,q)\in\Omega_1} \{\|\mathbf{w}_{p,q}\|_1 - \gamma_{p,q}^T (\Psi R_{p,q}\mathbf{x} - \mathbf{w}_{p,q}) \\ &+ \frac{\beta}{2} \|\Psi R_{p,q}\mathbf{x} - \mathbf{w}_{p,q}\|_2^2\} + \sum_{(i,j)\in\Omega_d} \{-\lambda_{i,j}^T (\Phi_{m,n} R_{i,j}\mathbf{x} - \mathbf{y}_{i,j}) \\ &+ \frac{\mu}{2} \|\Phi_{m,n} R_{i,j}\mathbf{x} - \mathbf{y}_{i,j}\|_2^2\}, \end{aligned} \qquad (9)$$

where β and μ are regularization parameters associated with quadratic penalty terms $\|\Psi R_{p,q}\mathbf{x} - \mathbf{w}_{p,q}\|_2^2$ and $\|\Phi_{m,n} R_{i,j}\mathbf{x} - \mathbf{y}_{i,j}\|_2^2$ respectively. $\gamma_{p,q}$ and $\lambda_{i,j}$ are the Lagrangian multipliers associated with the constraints $\Psi R_{p,q}\mathbf{x} = \mathbf{w}_{p,q}$ and

$\Phi_{m,n}R_{i,j} = \mathbf{y}_{i,j}$ respectively . The problem can be solved by solving (10) and (11) iteratively:

$$(\mathbf{w}_{p,q}^{k+1}, \mathbf{x}^{k+1}) = \arg\min_{\mathbf{w}_{p,q}^{k}, \mathbf{x}^{k}} L_A(\mathbf{w}_{p,q}^{k}, \mathbf{x}^{k}), \quad (10)$$

$$\begin{cases} \gamma_{p,q}^{k+1} = \gamma_{p,q}^{k} - \beta(\Psi R_{p,q}\mathbf{x}^k - \mathbf{w}_{p,q}^{k}) \\ \lambda_{i,j}^{k+1} = \lambda_{i,j}^{k} - \mu(\Phi_{m,n}R_{i,j}\mathbf{x}^k - \mathbf{y}_{i,j}). \end{cases} \quad (11)$$

Here, k is iteration number. We use alternating direction technique [7] [8] to decompose (10) into two sub-problems, each of which can be solved efficiently.

A. The $\mathbf{w}$ sub-problem

Given $\mathbf{x}$, the optimization problem associated with $\mathbf{w}_{p,q}$ can be expressed as:

$$\min_{\mathbf{w}_{p,q}} Q(\mathbf{w}_{p,q}) = \textstyle\sum_{(p,q)\in\Omega 1}\{\|\mathbf{w}_{p,q}\|_1 - \gamma_{p,q}^T(\Psi R_{p,q}\mathbf{x} - \mathbf{w}_{p,q}) + \frac{\beta}{2}\|\Psi R_{p,q}\mathbf{x} - \mathbf{w}_{p,q}\|_2^2\}. \quad (12)$$

The $\mathbf{w}$ sub-problem is separable with respect to:

$$\min_{\mathbf{w}_{p,q}} Q_1(\mathbf{w}_{p,q}) = \|\mathbf{w}_{p,q}\|_1 - \gamma_{p,q}^T(\Psi R_{p,q}\mathbf{x} - \mathbf{w}_{p,q}) + \frac{\beta}{2}\|\Psi R_{p,q}\mathbf{x} - \mathbf{w}_{p,q}\|_2^2. \quad (13)$$

The solution of every separated problem is a simple shrinkage operation [6]:

$$\mathbf{w}_{p,q} = \max\{|\Psi R_{p,q}\mathbf{x} - \tfrac{\gamma_{p,q}}{\beta}| - \tfrac{1}{\beta}, 0\} \otimes \operatorname{sgn}(\Psi R_{p,q}\mathbf{x} - \tfrac{\gamma_{p,q}}{\beta}), \quad (14)$$

where $\otimes$ stands for the element-wise product of two vectors.

B. The $\mathbf{x}$ sub-problem

With $\mathbf{w}_{p,q}$ fixed, the $\mathbf{x}$ sub-problem can be rewritten as:

$$\min_{\mathbf{x}} Q_2(\mathbf{x}) = \textstyle\sum_{(p,q)\in\Omega_1}\{-\gamma_{p,q}^T(\Psi R_{p,q}\mathbf{x} - \mathbf{w}_{p,q}) + \frac{\beta}{2}\|\Psi R_{p,q}\mathbf{x} - \mathbf{w}_{p,q}\|_2^2\} + \sum_{(i,j)\in\Omega_d}\{-\lambda_{i,j}^T(\Phi_{m,n}R_{i,j}\mathbf{x} - \mathbf{y}_{i,j}) + \frac{\mu}{2}\|\Phi_{m,n}R_{i,j}\mathbf{x} - \mathbf{y}_{i,j}\|_2^2\}. \quad (15)$$

(15) can be further represented as:

$$\min_{\mathbf{x}} Q_2(\mathbf{x}) = \textstyle\sum_{(p,q)\in\Omega 1}\{\frac{\beta}{2}\|\mathbf{x} - (\Psi R_{p,q})^{-1}(\mathbf{w}_{p,q} + \frac{\gamma_{p,q}}{\beta})\|_2^2\} + \sum_{(i,j)\in\Omega d}\{-\lambda_{i,j}^T(\Phi_{m,n}R_{i,j}\mathbf{x} - \mathbf{y}_{i,j}) + \frac{\mu}{2}\|\Phi_{m,n}R_{i,j}\mathbf{x} - \mathbf{y}_{i,j}\|_2^2\}. \quad (16)$$

We set $\mathbf{x}_0 = \sum_{(p,q)\in\Omega 1}(\Psi R_{p,q})^{-1}(\mathbf{w}_{p,q} + \frac{\gamma_{p,q}}{\beta})$, the sub-problem can be transformed to:

$$\min_{\mathbf{x}} Q_2(\mathbf{x}) = \tfrac{\beta}{2}\|\mathbf{x} - \mathbf{x}_0\|_2^2 + \textstyle\sum_{(i,j)\in\Omega d}\{-\lambda_{i,j}^T(\Phi_{m,n}R_{i,j}\mathbf{x} - \mathbf{y}_{i,j}) + \frac{\mu}{2}\|\Phi_{m,n}R_{i,j}\mathbf{x} - \mathbf{y}_{i,j}\|_2^2\}. \quad (17)$$

Clearly, $Q_2(u)$ is a quadratic function and its gradient can be expressed as:

$$g(\mathbf{x}) = \tfrac{d(Q_2(\mathbf{x}))}{dx} = \beta(\mathbf{x} - \mathbf{x}_0) + \textstyle\sum_{(i,j)\in\Omega_d}\{\mu(\Phi_{m,n}R_{i,j})^T (\Phi_{m,n}R_{i,j}\mathbf{x} - \mathbf{y}_{i,j}) - (\Phi_{m,n}R_i)^T\lambda_{i,j})\}. \quad (18)$$

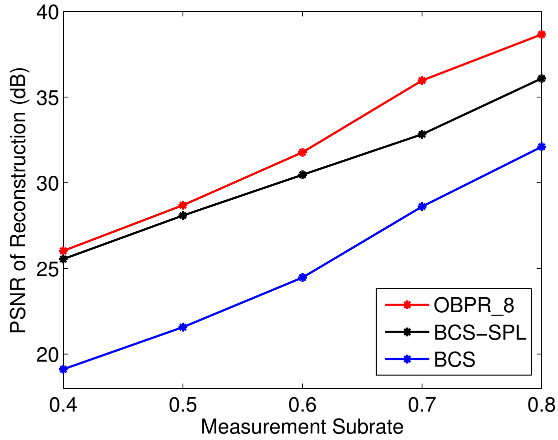

Fig. 3. PSNR vs Measurement Subrate for image $Vessels$

Setting $g(\mathbf{x}) = 0$ gives us the exact minimizer of Problem (15), that is:

$$\mathbf{x} = \{\beta I + \textstyle\sum_{(i,j)\in\Omega_d}\mu(\Phi_{m,n}R_{i,j})^T\Phi_{m,n}R_{i,j}\}^+ \{\beta\mathbf{x}_0 + \sum_{(i,j)\in\Omega_d}\{\mu(\Phi_{m,n}R_{i,j})^T\mathbf{y}_{i,j} + (\Phi_{m,n}R_{i,j})^T\lambda_{i,j}\}\}, \quad (19)$$

where M^+ stands for the Moore-Penrose pseudoinverse of matrix M^+. Computing the inverse or pseudoinverse at each iteration is too costly to implement. Here, the steepest descent method with the optimal step is used to solve Problem (15) iteratively by applying:

$$\hat{\mathbf{x}} = \mathbf{x} - \varepsilon g(\mathbf{x}), \quad (20)$$

where $\varepsilon = \text{abs}\{(g(\mathbf{x})^T g(\mathbf{x}))/(g(\mathbf{x})^T G g(\mathbf{x}))\}$ is the optimal $\varepsilon = \beta I + \sum_{(i,j)\in\Omega_d}\mu(\Phi_{m,n}R_{i,j})^T(\Phi_{m,n}R_{i,j})$, and I is the identity matrix.

IV. Experimental Results

In this section, OBPR is compared with two representative CS recovery methods, BCS method and BCS-SPL method, which deal with the image signal in DCT domain.

The curve of PSNR versus measurement subrate from 0.4 to 0.8 of image $Vessels$ (size=96×96, D=16, d=8) for the three different approaches is plotted in Fig. 3. We can find the performance of OBPR is consistently superior to the other two methods. Additionally, some reconstructed images are shown in Fig. 4 (measurement subrate=60%). We can see the blocking artifacts of the image reconstructed by BCS. The reconstructed image by OBPR is better than that of BCS-SPL.

Tables I lists more results of different images (D=16, d=8). Results present the similar conclusion that the performance of OBPR is better than that of BCS and BCS-SPL methods. In addition, we can find OBPR has more prominent advantage at higher measurement rate. Other reconstructed images are not listed here due to limited space.

Further, considering the influence of overlap degree on experiment result, we set different overlap degrees in the

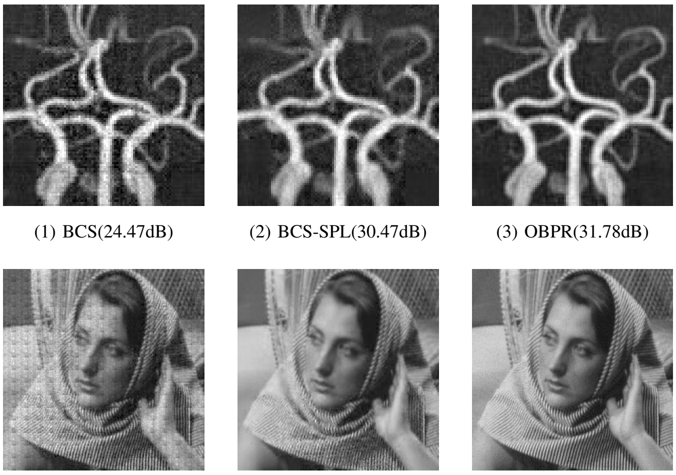

(1) BCS(24.47dB) (2) BCS-SPL(30.47dB) (3) OBPR(31.78dB)

(4) BCS(24.54dB) (5) BCS-SPL(30.33dB) (6) OBPR(32.16dB)

Fig. 4. Some images reconstructed by three different approaches

TABLE I
PSNR VS MEASUREMENT SUBRATE FOR IMAGE $Vessels$, $Barbara$ AND $Leaves$

$Vessels(96 \times 96)$					
Algorithm	Measurement Subrate				
	0.4	0.5	0.6	0.7	0.8
BCS	19.12	21.57	24.47	28.61	32.10
BCS-SPL	25.55	28.09	30.47	32.83	36.09
OBCS_8	26.03	28.69	31.78	35.97	38.66
$Barbara(256 \times 256)$					
Algorithm	Measurement Subrate				
	0.4	0.5	0.6	0.7	0.8
BCS	18.98	21.36	24.54	27.30	31.08
BCS-SPL	26.86	28.90	30.33	32.88	36.33
OBCS_8	26.94	29.19	32.16	35.29	38.18
$Leaves(256 \times 256)$					
Algorithm	Measurement Subrate				
	0.4	0.5	0.6	0.7	0.8
BCS	15.42	17.91	21.32	23.96	27.29
BCS-SPL	24.54	26.40	28.42	30.78	33.17
OBCS_8	24.85	27.52	29.48	32.09	34.35

experiment (d=8, d=4). Tables II lists the results for image $Vessels$ and $Leaves$. We can see that the reconstruction quality is improved along with overlap degree increase.

V. CONCLUSION

In this paper, we propose a new image compressive sensing scheme using overlapped block projection and reconstruction (OBPR). Different from traditional methods, the sampling of image is applied on overlapped blocks. In process of reconstruction, an efficient augmented Lagrangian based technique is exploited to solve the proposed optimization problem. Experimental results manifest that OBPR is able to provide a significant gain in reconstruction quality over BCS and BCS-SPL.

TABLE II
PSNR VS MEASUREMENT SUBRATE FOR IMAGE $Vessels$ AND $Leaves$

$Vessels(96 \times 96)$					
Algorithm	Measurement Subrate				
	0.4	0.5	0.6	0.7	0.8
OBCS_8	26.03	28.69	31.78	35.97	38.66
OBCS_4	26.64	29.73	33.06	36.55	39.28
$Leaves(256 \times 256)$					
Algorithm	Measurement Subrate				
	0.4	0.5	0.6	0.7	0.8
OBCS_8	24.85	27.52	29.48	32.09	34.35
OBCS_4	25.35	28.40	31.18	33.52	36.57

There are many issues that future work should consider. The sparsity degree of a signal in transform domain plays a significant role in recovery while this paper simply chooses discrete cosine transform. We can try to seek a domain in which the signal has a higher degree of sparsity in future works to achieve better performance, such as [11] [12].

REFERENCES

[1] D. L. Donoho, "Compressed sensing," *IEEE Transaction on Information Theory*, 2006, 52(4): 1289–1306.

[2] J. Zhang, D. Zhao, C. Zhao, R. Xiong, S. Ma and W. Gao, "Compressed sensing recovery via collaborative sparsity," *IEEE Data Compression Conference (DCC)*, pp. 287–296, Apr. 2012.

[3] J. Zhang, D. Zhao, F. Jiang, W. Gao, "Structural group sparse representation for image compressive sensing recovery," *IEEE Data Compression Conference (DCC)*, pp. 331–340, Mar. 2013.

[4] L. Gan, "Block Compressed Sensing of Natural Images," *Digital Signal Processing*, July 2007, pp. 403–406.

[5] M. Sungkwang and J. F. Fowler, "Block compressed sensing of images using directional transforms," *Image Processing (ICIP), 2009 16th IEEE International Conference on*, pp. 3021–3024, Nov. 2009.

[6] X. Zhang, R. Xiong, S. Ma and W. Gao, "Reducing Blocking Artifacts in Compressed Images via Transform-Domain Non-local Coefficients Estimation," *Multimedia and Expo (ICME), 2012 IEEE International Conference on*, vol. no. pp. 836–841, July 2012.

[7] X. Zhang, R. Xiong, X. Fan, S. Ma and W. Gao, "Compression Artifact Reduction by Overlapped-Block Transform Coefficient Estimation With Block Similarity," *Image Processing, IEEE Transactions on*, vol. 22, no. 12, pp. 4613–4626, Dec. 2013.

[8] M. V. Afonso, J. M. Bioucas-Dias and M. A. Figueiredo, "Fast image recovery using variable splitting and constrained optimization," *IEEE Transactions on Image Processing*, vol. 19, no. 9, pp. 2345–2356, Sep. 2010.

[9] J. F. Cai, S. Osher and Z. W. Shen, "Split Bregman methodsand frame based image restoration," *Multiscale Model. Simul.*, vol. 8. pp. 5057–5071, 2009.

[10] J. Zhang, D. Zhao, C. Zhao, R. Xiong, S. Ma and W. Gao, "Image compressive sensing recovery via collaborative sparsity," *Emerging and Selected Topics in Circuits and Systems, IEEE Journal on*, vol. 2, no. 3, pp. 380–391, Sep. 2012.

[11] J. Zhang, C. Zhao, D. Zhao, and W. Gao, "Image compressive sensing recovery using adaptively learned sparsifying basis via L0 minimization," *Signal Processing*, vol. 103, pp. 114–126, 2014.

[12] J. Zhang, D. Zhao, and W. Gao, "Group-based sparse representation for image restoration," *Image Processing, IEEE Transactions on*, vol. 23, no. 8, pp. 3336–3351, Aug. 2014.